Review of Scientific Instruments

Neutron-induced signal on the single crystal chemical vapor deposition diamond-based neutral particle analyzer

Cite as: Rev. Sci. Instrum. **91**, 113304 (2020); https://doi.org/10.1063/5.0020460
Submitted: 01 July 2020 • Accepted: 29 October 2020 • Published Online: 12 November 2020

S. Kamio, Y. Fujiwara, K. Ogawa, et al.

Review of Scientific Instruments ARTICLE scitation.org/journal/rsi

Neutron-induced signal on the single crystal chemical vapor deposition diamond-based neutral particle analyzer

Cite as: Rev. Sci. Instrum. 91, 113304 (2020); doi: 10.1063/5.0020460
Submitted: 1 July 2020 • Accepted: 29 October 2020 •
Published Online: 12 November 2020

S. Kamio,[1,a)] Y. Fujiwara,[1] K. Ogawa,[1,2] M. I. Kobayashi,[1] S. Sangaroon,[1,3] M. Isobe,[1,2] R. Seki,[1,2] H. Nuga,[1] M. Osakabe,[1,2] S. Matsuyama,[4] M. Miwa,[4] and S. Toyama[4]

AFFILIATIONS

[1]National Institute for Fusion Science, 322-6 Oroshi-cho, Toki 509-5292, Japan
[2]The Graduate University for Advanced Studies SOKENDAI, 322-6 Oroshi-cho, Toki 509-5292, Japan
[3]Mahasarakham University, 20-41 Kamriang, Kantharawichai, Mahasarakham 44150, Thailand
[4]Tohoku University, 6-6 Aoba, Aramaki, Aoba-ku, Sendai 980-8579, Japan

[a)]**Author to whom correspondence should be addressed:** kamio@nifs.ac.jp

ABSTRACT

A diamond-based neutral particle analyzer (DNPA) array composed of single-crystal chemical vapor deposition (sCVD) diamond detectors was installed on the Large Helical Device (LHD) for measuring the helically trapped energetic particles. In high neutron flux experiments, the unwanted neutron-induced pulse counting rate should be estimated using the neutron diagnostics because a diamond detector is sensitive to neutrons as well as energetic neutral particles. In order to evaluate the quantitative neutron-induced pulse counting rate on the DNPA, the response functions of the sCVD diamond detector for mono-energetic neutrons were obtained using accelerator-based D–D and D–^{7}Li neutron sources in Fast Neutron Laboratory (FNL). As a result of the neutron flux estimation by the Monte Carlo N-Particle code at the NPA position in the LHD and the response function obtained in the FNL experiment, the counting rate of the neutron-induced signal was predicted to be 1.1 kcps for the source neutron emission rate of $S_n = 1 \times 10^{15}$ n/s. In the LHD experiment, the neutron-induced signals were observed by closing the gate valve during the plasma discharges. It is found that the counting rates of the neutron-induced signals proportional to S_n reached 1.1 kcps at $S_n = 1 \times 10^{15}$ n/s. As a result of the quantitative estimation of the neutron-induced signals on the DNPA using other neutron measurements, it has become possible to accurately measure energetic neutral particles in the high neutron flux experiment.

I. INTRODUCTION

In the future fusion reactor, alpha particles should be well confined and used for plasma heating to sustain steady state without external heating. Therefore, it is very important to study the confinement physics of energetic particles because the energetic particles can cause magnetohydrodynamic (MHD) instabilities that transport the energetic particles, deteriorating their confinement. In order to investigate the behavior of the energetic particles in the experimental devices for fusion research, a neutral particle analyzer (NPA) has been developed.[1] Some of the energetic particles inside the plasma undergo charge exchange with the neutral particles and are lost from the magnetic confinement. The energy spectrum of the lost energetic particles can be observed with the NPA along the line of sight. A silicon-diode detector is widely used because of the good energy resolution and a size small enough to make an array.[2–6] However, high neutron irradiation likely causes permanent damage to the semiconductor. Since the silicon-diode detector cannot be used in burning plasma, a diamond detector, which has sufficient neutron radiation hardness, has been developed.[7–9] On the other hand, in the experiment using deuterium gas, the neutron emission produced by the D–D fusion reaction is also used for investigating the behavior of the energetic particles because the neutron emission rate depends on the spatial and energy distribution functions of energetic

particles. Therefore, by measuring the energetic particles in the hard neutron radiation experiments, comprehensive investigation can be done together with the neutron measurement. The result of the NPA is useful because the energy spectrum of the energetic particles can be obtained.

In the Large Helical Device (LHD), confinement of the energetic particles in a helical ripple is studied for understanding the confinement physics in a three-dimensional magnetic configuration because the transport of the helically trapped energetic particles is one of the important issues for the helical confinement system. In the LHD, the deuterium plasma experiment was started in 2016, and the neutron diagnostics were installed for the study of the energetic particles by D–D fusion reaction.[10,11] In order to measure the energetic particles in the hard neutron radiation experiment, a single-crystal chemical vapor deposition (sCVD) diamond-based NPA (DNPA) was developed for measuring the helically trapped energetic particles in the LHD.[12] Diamond was adopted because of its high radiation hardness. Actually, the sCVD diamond detectors have been used as the neutron diagnostic for the hard neutron radiation experiments.[13,14] Using the DNPA, energy spectra of the energetic particles were observed with high energy resolution in high neutron emission experiments. By measuring in the high neutron emission experiment, the DNPA can be used together with the neutron diagnostics[15,16] as well as with the other NPAs[17,18] and spectroscopic measurements.[19,20] By measuring with other energetic particle diagnostics, a better understanding of fast particle energy and spatial distributions is expected. The DNPA also detects the neutron-induced signals during the discharge in the deuterium experiment. However, the quantitative neutron-induced signals on the DNPA have not been evaluated yet. As the diagnostic for the energetic neutral particle, the neutron-induced signals should be estimated from the neutron measurement.

In this paper, we show the results of the neutron-induced signals on the sCVD diamond detectors for the NPA. The DNPA system configuration is shown in Sec. II. Section III shows the observed energy spectra by the neutron irradiation experiments in Fast Neutron Laboratory (FNL). Quantitative evaluation of the neutron-induced signal on the diamond detector was observed in FNL. In Sec. IV, the results in the LHD experiments are shown. The neutron-induced signal on the DNPA was measured experimentally. In addition, the typical experimental results are shown with the neutron-induced signal estimation. Section V is the summary.

II. DNPA SYSTEM CONFIGURATION

The schematic view of the circuit of the DNPA is shown in Fig. 1. The sCVD diamond B12[21] made by CIVIDEC is used as the detector of the DNPA.[12] The sCVD diamond has 4.5 × 4.5 mm^2 area and 0.5 mm thickness, while the electrode has 4.0 × 4.0 mm^2 area and 100 nm thickness, made of titanium. The bias voltage is 400 V. In the case of plasma diagnostics in fusion research, the typical energy of the positive ion source neutral beam injection (NBI) is in the range of 40 keV–80 keV. In order to measure the 40 keV –80 keV energy signals, the preamplifier 2001A and the shaping amplifier 2026× made by CANBERRA were used to achieve high multiplication. The typical gain of the amplifier is 750 for the plasma measurement. The corresponding energy of the thermal noise was

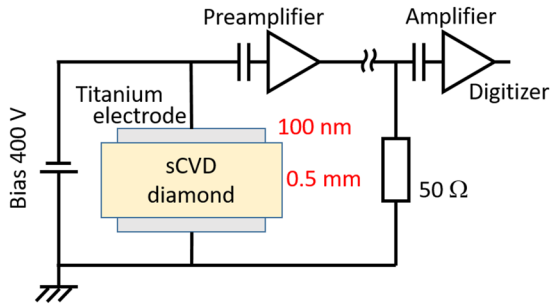

FIG. 1. The schematic view of the circuit of the DNPA.

less than ~30 keV. Therefore, the typical energy range of the DNPA is 30 keV–600 keV for the plasma measurement. In order to perform calibration, an ^{241}Am alpha source was used. The gain of the amplifier is 75 for the calibration. The digitizer WE7562 for pulse height analysis made by YOKOGAWA is used for counting the signals. The detector measures the pulse height in the range of 0 V–10 V. The maximum energy of the DNPA measurement range corresponds to 10 V. The pulse length of the signal is ~1 μs in the counting time window of 10 ms. Therefore, in order to avoid the pile-up, the DNPA should be used with the counting rate of less than 100 kcps. The counting loss rate due to the dead-time of the detector[22] is 10% of the true count under 100 kcps.

III. NEUTRON IRRADIATION IN FNL

In order to quantitatively measure the neutron-induced signal on the DNPA, fast neutron irradiation experiments have been carried out in Fast Neutron Laboratory (FNL)[23,24] at Tohoku University. Figure 2 shows the schematic view of the FNL experiments. The accelerated deuteron DC beam by the Dynamitron accelerator is delivered to the target with the energy E_{beam}. Deuterium gas or solid lithium was used as the target. The neutrons produced by D(d,n)^{3}He or by ^{7}Li(d,n)^{8}Be reactions arrive at the sCVD diamond detector with the energy of $E_n + E_{beam}\cos\alpha$. E_n of 2.45 MeV with D(d,n)^{3}He reaction was used for evaluating the neutron-induced signals in the D–D fusion plasma experiment, and E_n of 15.0 MeV with ^{7}Li(d,n)^{8}Be reaction was used for measuring the neutrons with the DNPA.

The deuterium gas target was used for measuring the neutron counting rate by 2.45 MeV D–D fusion reaction. In the case of using the gas target, the energy loss of the accelerated deuteron at the 6.4 μs Harbor foil should be considered. The detector was installed at l = 35 mm and α = 20°. 20 m cables for connecting the

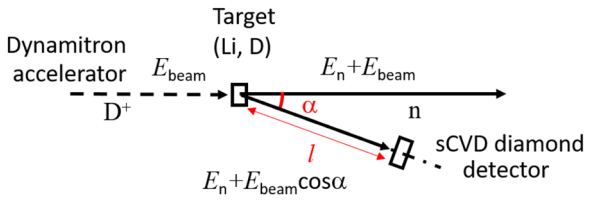

FIG. 2. Schematic view of the FNL experiments.

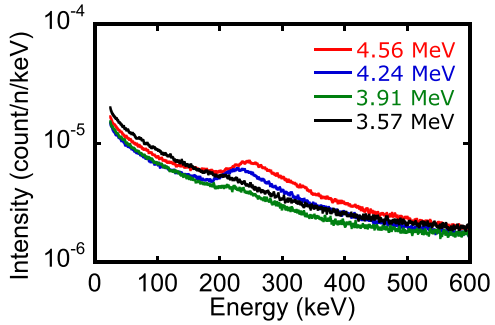

FIG. 3. The pulse height spectrum of the DNPA counting rate of the neutron irradiation experiments using the D–D neutron source.

amplifiers were used for reproducing the experimental conditions. Figure 3 shows the energy distributions of the DNPA counting rate during the neutron irradiation experiment. The irradiated neutron energy was 3.57 MeV–5.52 MeV with the acceleration voltage of 2.1 MV–3.0 MV. Here, the beam energies E_{beam} attenuated by the Harbor foil become 1.34 MeV–2.43 MeV when the acceleration voltages are 2.1 MV–3.0 MV. The neutron irradiation time was 20 min for each energy. The observed count divided by the neutron fluence was ~4.8×10^{-4} count/(n/cm^2) with the energy range of 50 keV–600 keV. A characteristic peak was observed at 200 keV–300 keV. Although the reason for the appearance of the peak is not clear, the calculation of elastic scattering inside the diamond due to the neutron irradiation by the PHITS code[25] shows a similar result in this energy range. Therefore, we expect the energy spectrum of the DNPA due to 2.45 MeV neutrons to be comparable to the one shown in Fig. 3.

Figure 4 shows the results of the experiment with the D–^{7}Li neutron source measured with the wide energy range. In order to measure the high energy neutrons, the gain of the amplifier is decreased to 50. The irradiated neutron energies were 15.89 MeV, 16.99 MeV, and 17.68 MeV with the acceleration voltage of 1.5 MV, 2.4 MV, and 3.0 MV, respectively. As a result of neutron irradiation, characteristic energy distributions were observed. The

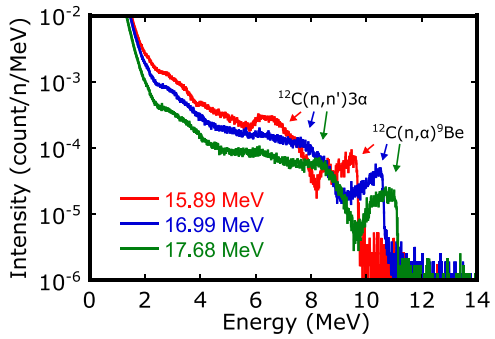

FIG. 4. The pulse height spectrum of the DNPA counting rate of the neutron irradiation experiments with the irradiation energy of 15.89 MeV, 16.99 MeV, and 17.68 MeV using the D–^{7}Li neutron source.

edge of ^{12}C(n,α)^{9}Be and ^{12}C(n,n′)3α could be identified by the DNPA.

IV. EXPERIMENTS IN LHD

In the LHD, the DNPA was developed for measuring the energetic particles that were accelerated by ion cyclotron range of frequency (ICRF) waves or injected by perpendicular-neutral beam (p-NB) injectors. The DNPA measurement lines of sight with the LHD poloidal cross section are shown in Fig. 5. The lines of sight of Ch1 and of Ch7 are across the lower and upper helical ripples, and the line of sight of Ch4 is across the magnetic axis. Because the direction of the measurement lines of sight is perpendicular to the magnetic field lines, Ch1 and Ch7 are expected to observe the helical ripple trapping particles. The DNPA counting rate is expected to be high during the p-NB injection. On the other hand, the neutron emission rate is high during the tangential-neutral beam (t-NB) injection because the injection energy of the t-NBs is higher than the injection energy of p-NBs. The typical injection energy of t-NB (NB Nos. 1–3) is 130 keV–180 keV, and the typical injection energy of *p*-NB (NB Nos. 4 and 5) is 60 keV–80 keV.

The diamond detectors were installed at the basement of the LHD torus hall. Three meter straight pipes were used to extend the vacuum chamber from the LHD lower side port. In order to reduce the neutron effect, the diamond detectors are located under the floor slab through 1.5 m heavy concrete with 5 cm inner diameter pipes. The detectors are located at ~7.8 m below the magnetic axis of the torus plasma. The neutron flux was calculated by the Monte Carlo N-Particle (MCNP) transport code.[26,27] The neutron flux at the position of the detectors was evaluated as 2.4×10^6 n/cm^2/s when the neutron source emission rate is 1×10^{15} n/s.[28] The neutron source emission rate S_n is measured with the neutron flux monitor.[29] Considering the estimated sensitivity of the diamond detector to the neutron of 4.8×10^{-4} count/(n/cm^2) with the energy range of

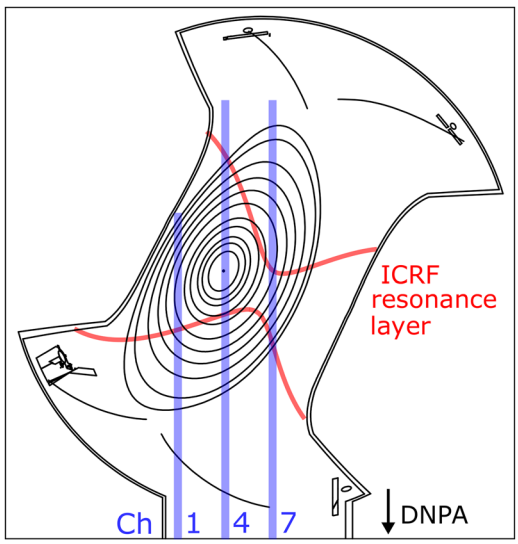

FIG. 5. The lines of sight of the DNPA together with the plasma flux surface and the ICRF resonance layers in the LHD poloidal cross section.

50 keV–600 keV in the FNL experiment in Fig. 3, the counting rate predicted by using S_n is 1.1 kcps during the LHD experiment with $S_n = 1 \times 10^{15}$ n/s.

Figure 6 shows the experimental result of the neutron-induced signal measurement. During the discharges with the high neutron emission rate, the DNPA measured signals other than the neutral particles by closing the gate valve. The gate valve, which is made of stainless steel, prevents neutral particles from passing through. 49 discharges with a high S_n rate of up to 2.5×10^{15} n/s were used for neutron-induced signal measurement. In this experiment, the signals are not only neutron-induced signals but also the signals induced by the gamma rays. These signals cannot be identified with the DNPA. However, estimation of the signals other than the energetic neutral particles is important for measuring energetic neutral particles. As shown in Fig. 6(a), the energy integrated neutron signals were clearly proportional to S_n. The counting rate coefficients of three DNPA channels were almost the same. As a result of linear fitting, the DNPA average counting rate for S_n was 1.1 kcps when $S_n = 10^{15}$ n/s. The observed counting rate of 1.1 kcps was consistent with the prediction. This result also indicates that the calculation of the neutron flux rate at the basement by MCNP of 2.4×10^6 n/cm^2/s at $S_n = 10^{15}$ n/s was reasonable. The energy distributions of each channel are shown in Fig. 6(b). A peak of the neutron-induced signal shaped similar to the result in the FNL experiment shown in Fig. 3 was observed at around 300 keV. These results can be used for estimation of the counting rate of the neutron-induced signal during the neutral particle measurement. The quantitative neutron-induced signal can be estimated by multiplying S_n to the results shown in Fig. 6 during the experiment.

Typical experimental results obtained by measuring the energetic neutral particles in the LHD are shown in Figs. 7 and 8. Figure 7(a) shows the time evolutions of injection powers, Fig. 7(b) shows the plasma density and temperatures, and Fig. 7(c) shows the total neutron emission rate S_n. In this discharge, p-NB and t-NB are used as the energetic particle sources, and ICRF heating is used to accelerate ions. The highest S_n is 1.1×10^{15} n/s at the timing of t-NB injection. Figures 7(d)–7(f) show the energy integrated counting rates of the DNPA (red lines) and the estimated neutron-induced signal (green lines) of each channel. The difference between the total signal and the estimation of the neutron-induced signal is the signal of the energetic neutral particles. The highest counting rate was less than 30 kcps at the timing of p-NB injection. The p-NB modulation pulses, which were injected with the energy of 59 keV, can be clearly confirmed on DNPA Ch1 and Ch7. On the other hand, the counting rate of Ch4 was lower than the counting rate of Ch1 and of Ch7. This difference indicates that the p-NB particles were trapped in a helical ripple, and the energetic neutral particles were successfully observed with the DNPA. In the case of Ch4, the counting rate was close to the estimation of the counting rate of the neutron-induced signal. The total counting rate of Ch1 was higher than the counting rate of Ch7 during the p-NB injection. However, during the timing of ICRF injection of 5.3 s–6.3 s, the counting rate of Ch7 was higher than that of Ch1. This count of Ch7 may be the accelerated particles

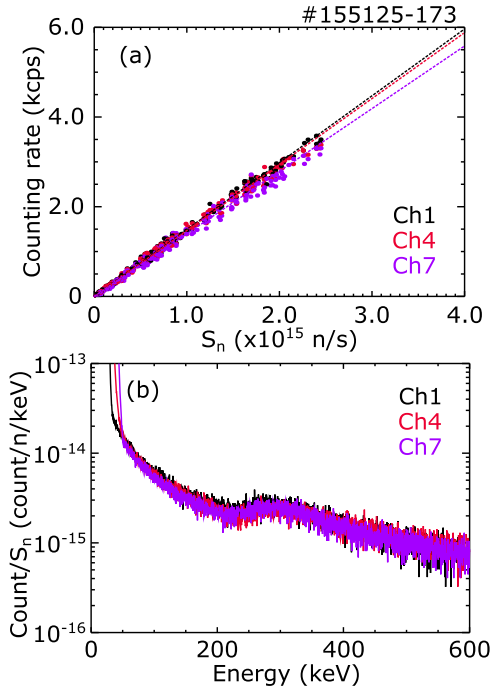

FIG. 6. (a) The DNPA integrated counting rates of 50 keV–600 keV during the discharges with the gate valve closed. (b) The pulse height spectrum of each channel. The counting rates are normalized to 10^{15} neutrons.

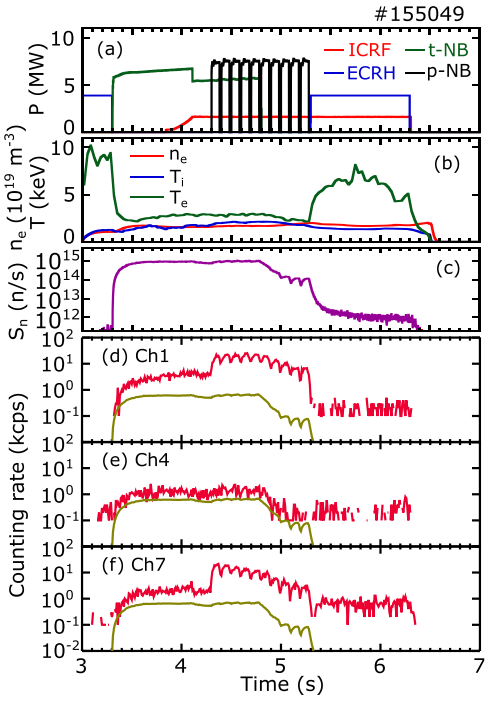

FIG. 7. Time evolutions of (a) the injection powers for plasma start-up, sustaining, and heating, (b) the electron density and the temperatures of the ion and electron, (c) the total neutron emission rate, and (d)–(f) the counting rates of each DNPA channel at 50 keV–300 keV (red lines) and the estimated neutron-induced signal (green lines).

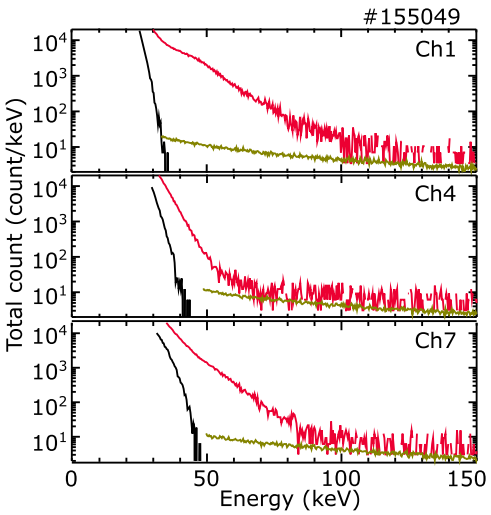

FIG. 8. The pulse height spectrum of the total count (red lines), the estimated neutron-induced signal (green lines), and the thermal noise (black lines) of each channel.

at the ICRF resonance layers on the Ch7 line of sight shown in Fig. 5. The estimated neutron-induced signal of this timing was negligible. As shown in Figs. 7(d)–7(f), the difference between the lines of sight clearly appeared for DNPA Ch1, Ch4, and Ch7.

The energy distributions of the discharge are shown in Fig. 8. Red lines are the total count during 3 s–7 s shown in Fig. 7. Black lines are the thermal noise estimated before the plasma start-up in the same discharge. Green lines are the spectra of the neutron-induced signal estimated using the energy distributions of Fig. 6(b). The counting rate of the neutral particles was much higher than the neutron-induced signal at the lower energy region. However, the neutral counting rate was almost the same with the neutron-induced signal at more than 100 keV, 70 keV, and 90 keV for Ch1, Ch4, and Ch7, respectively. The estimation of the neutron noise was very important for discussing the confinement of energetic particles in the high energy region.

The energy components higher than the p-NB energy of 59 keV are considered to be the scattered t-NB particles, which were injected with the energies of 153 keV (NB No. 1), 170 keV (NB No. 2), and 170 keV (NB No. 3), or the particles accelerated by ICRF heating. We will clarify the confinement physics generated by p-NB injection and/or ICRF heating using the DNPA by changing the experimental conditions in the LHD.

V. SUMMARY

The NPA array using sCVD diamond detectors was developed in the LHD deuterium experiments for measuring the helically trapped energetic particles. In order to measure the quantitative neutron-induced signals on the DNPA, mono-energetic neutrons were irradiated to the sCVD diamond detector in FNL. As a result of the FNL experiments and the neutron flux estimation by MCNP, the neutron-induced signal was estimated to be 1.1 kcps during plasma discharges with the total neutron emission rate of $S_n = 10^{15}$ n/s in the LHD. This counting rate is low enough to measure the neutral particles in the high neutron emission experiments. The characteristic peak was observed at around 200 keV, and the peak was shifted by changing the energy of irradiated neutrons. The characteristic energy spectra of fast neutron signals were also observed with diamond detectors with a wide energy range in the FNL experiment. In the LHD, the neutron-induced signals were measured by closing the gate valve during the plasma discharges. The amount of signal due to the neutron results in a linear relation with the neutron emission. The counting rate of the neutron-induced signal was 1.1 kcps when $S_n = 10^{15}$ n/s. This counting rate is the same as the predicted one. Using the results of the neutron measurement, the neutron-induced signal was estimated quantitatively during the experiment for measuring the energetic neutral particles. The counting rate due to neutrons was estimated to be much lower than the signal of the neutral particles even during the neutron emission rate of 10^{15} n/s, which is the highest neutron emission rate in LHD experiments.

ACKNOWLEDGMENTS

The authors wish to thank the support of the LHD experiment group in performing the experiments. This work was supported by the NINS Program for Cross-Disciplinary Study (Grant No. 0131190), the NIFS Collaboration Research Program (Grant Nos. KOAH037 and KOAA001), and the NIFS (Grant Nos. ULRR006, ULRR035, and ULRR703).

DATA AVAILABILITY

The data that support the findings of this study are available from the corresponding author upon reasonable request.

REFERENCES

[1] D. D. R. Summers, R. D. Gill, and P. E. Stott, J. Phys. E: Sci. Instrum. **11**, 1183 (1978).
[2] Y. Miura, H. Takeuchi, and Y. Ohara, Rev. Sci. Instrum. **56**, 1111 (1985).
[3] M. Osakabe, T. Yamamoto, Y. Takeiri, T. Mutoh, E. Asano, K. Ikeda, K. Tsumori, O. Kaneko, K. Kawahata, N. Ohyabu *et al.*, Rev. Sci. Instrum. **72**, 788–791 (2001).
[4] V. Tang, J. Liptac, R. R. Parker, P. T. Bonoli, C. L. Fiore, R. S. Granetz, J. H. Irby, Y. Lin, S. J. Wukitch, AlcatorC-Mod Team *et al.*, Rev. Sci. Instrum. **77**, 083501 (2006).
[5] J. Kalliopuska, F. García, M. Santala, S. Eränen, S. Karttunen, T. Virolainen, T. Kovero, T. Vehmas, and R. Orava, Nucl. Instrum. Methods Phys. Res., Sect. A **591**, 92–97 (2008).
[6] S. H. Kim, J. G. Kwak, C. K. Hwang, S. J. Wang, and H. J. Lee, Fusion Eng. Des. **86**, 1236–1238 (2011).
[7] M. Isobe, Y. Kusama, M. Takechi, T. Nishitani, and A. Morioka, Rev. Sci. Instrum. **72**, 611 (2001).
[8] A. G. Alekseyev, D. S. Darrow, A. L. Roquemore, and S. S. Medley, Rev. Sci. Instrum. **74**, 1905 (2003).
[9] A. V. Krasilnikov, S. S. Medley, N. N. Gorelenkov, R. V. Budny, O. V. Ignatyev, Y. A. Kaschuck, M. P. Petrov, and A. L. Roquemore, Rev. Sci. Instrum. **70**, 1107 (1999).
[10] M. Isobe, K. Ogawa, T. Nishitani, H. Miyake, T. Kobuchi, N. Pu, H. Kawase, E. Takada, T. Tanaka, S. Li *et al.*, IEEE Trans. Plasma Sci. **46**, 2050–2058 (2018).
[11] H. Nuga, R. Seki, K. Ogawa, S. Kamio, Y. Fujiwara, M. Osakabe, M. Isobe, T. Nishitani, M. Yokoyama, and LHD Experiment Group, Plasma Fusion Res. **14**, 3402075 (2019).

[12]S. Kamio, Y. Fujiwara, K. Ogawa, M. Isobe, R. Seki, H. Nuga, T. Nishitani, M. Osakabe, and LHD Experiment Group, J. Instrum. **14**, C08002 (2019).
[13]M. Angelone, D. Lattanzi, M. Pillon, M. Marinelli, E. Milani, A. Tucciarone, G. Verona-Rinati, S. Popovichev, R. M. Montereali, M. A. Vincenti *et al.*, Nucl. Instrum. Methods Phys. Res., Sect. A **595**, 616–622 (2008).
[14]M. I. Kobayashi, M. Angelone, S. Yoshihashi, K. Ogawa, M. Isobe, T. Nishitani, S. Sangaroon, S. Kamio, Y. Fujiwara, T. Tsubouchi *et al.*, Fusion Eng. Des. **161**, 112063 (2020).
[15]M. Isobe, K. Ogawa, T. Nishitani, N. Pu, H. Kawase, R. Seki, H. Nuga, E. Takada, S. Murakami, Y. Suzuki *et al.*, Nucl. Fusion **58**, 082004 (2018).
[16]K. Ogawa, M. Isobe, T. Nishitani, S. Murakami, R. Seki, H. Nuga, S. Kamio, Y. Fujiwara, H. Yamaguchi, Y. Saito *et al.*, Nucl. Fusion **59**, 076017 (2019).
[17]Y. Fujiwara, S. Kamio, K. Ogawa, H. Yamaguchi, R. Seki, H. Nuga, T. Nishitani, M. Isobe, and M. Osakabe, J. Instrum. **15**, C02021 (2020).
[18]T. Ozaki, P. Goncharov, E. Veshchev, N. Tamura, S. Sudo, T. Seki, H. Kasahara, Y. Takase, and T. Ohsako, Rev. Sci. Instrum. **79**, 10E518 (2008).
[19]Y. Fujiwara, S. Kamio, H. Yamaguchi, A. V. Garcia, L. Stagner, H. Nuga, R. Seki, K. Ogawa, M. Isobe, M. Yokoyama *et al.*, Plasma Fusion Res. **14**, 3402129 (2019).
[20]Y. Fujiwara, S. Kamio, H. Yamaguchi, A. V. Garcia, L. Stagner, H. Nuga, R. Seki, K. Ogawa, M. Isobe, M. Yokoyama *et al.*, Nucl. Fusion **60**, 112014 (2020).
[21]See https://cividec.at/ for CIVIDEC Instrumentation GmbH. Austria.
[22]J. W. Müller, Nucl. Instrum. Methods **112**, 47–57 (1973).
[23]M. Baba, M. Takada, T. Iwasaki, S. Matsuyama, T. Nakamura, H. Ohguchi, T. Nakao, T. Sanami, and N. Hirakawa, Nucl. Instrum. Methods Phys. Res., Sect. A **376**, 115–123 (1996).
[24]M. Sasaki, T. Nakamura, N. Tsujimura, O. Ueda, and T. Suzuki, Nucl. Instrum. Methods Phys. Res., Sect. A **418**, 465–475 (1998).
[25]T. Sato, Y. Iwamoto, S. Hashimoto, T. Ogawa, T. Furuta, S.-i. Abe, T. Kai, P.-E. Tsai, N. Matsuda, H. Iwase *et al.*, J. Nucl. Sci. Technol. **55**, 684–690 (2018).
[26]*MCNP6 Users Manual*, edited by D. B. Pelowits (Los Alamos National Laboratory, Los Alamos, 2013), LA-CP-13-00634.
[27]T. Nishitani, K. Ogawa, and M. Isobe, Fusion Eng. Des. **123**, 1020–1024 (2017).
[28]S. Sangaroon, K. Ogawa, M. Isobe, M. I. Kobayashi, Y. Fujiwara, S. Kamio, R. Seki, H. Nuga, H. Yamaguchi, M. Osakabe, and LHD Experiment Group, Rev. Sci. Instrum. **91**, 083505 (2020).
[29]M. Isobe, K. Ogawa, H. Miyake, H. Hayashi, T. Kobuchi, Y. Nakano, K. Watanabe, A. Uritani, T. Misawa, T. Nishitani *et al.*, Rev. Sci. Instrum. **85**, 11E114 (2014).